International Journal of Pharmaceutics 383 (2010) 228–235

Contents lists available at ScienceDirect

International Journal of Pharmaceutics

journal homepage: www.elsevier.com/locate/ijpharm

Pharmaceutical Nanotechnology

Transfection efficiencies of PAMAM dendrimers correlate inversely with their hydrophobicity

Antos Shakhbazau[a], Iauhenia Isayenka[a], Nikolai Kartel[a], Natalya Goncharova[b], Ihar Seviaryn[b], Svetlana Kosmacheva[b], Mihail Potapnev[b], Dzmitry Shcharbin[c,*], Maria Bryszewska[d]

[a] Institute of Genetics and Cytology of Natl. Acad. Sci. Bel., Minsk, Belarus
[b] Republic Centre for Haematology and Transfusiology, Minsk, Belarus
[c] Institute of Biophysics and Cellular Engineering of Natl. Acad. Sci. Bel., Akademicheskaja, 27, 220072 Minsk, Belarus
[d] Department of General Biophysics, University of Lodz, Lodz, Poland

ARTICLE INFO

Article history:
Received 18 June 2009
Received in revised form
10 September 2009
Accepted 11 September 2009
Available online 19 September 2009

Keywords:
Dendrimer
Gene delivery
Transfection
Dendriplex
Ethidium bromide intercalation assay
ANS fluorescence

ABSTRACT

Dendriplexes were characterized by ethidium bromide intercalation assay and their transfection efficiency was studied using HEK 293 cells and human mesenchymal stem cells. PAMAM G4 showed a higher transfection efficiency than PAMAM G3–G6, G4-OH, G4-25% or G4-50% dendrimers. Substitution of OH groups for the NH_2 surface groups rendered the dendrimer unable to form dendriplexes and to transfect cells. Partial (25%) substitution of CH_3 groups for the NH_2 groups markedly impaired transfection; 50% substitution decreased the ability of PAMAM G4 to transfect threefold. It was concluded that increased hydrophobicity decreased the ability of dendrimers to transfect. PAMAM G4-50% is highly hydrophobic and forms micelles in solution, which can transfect pGFP. The results of ethidium bromide intercalation assays, ANS fluorescence studies and transfection efficiencies of PAMAM dendrimers were correlated. Subsequently, we constructed a neurotrophin-encoding plasmid and studied its delivery to mesenchymal stem cells using PAMAM G4 dendrimer and Lipofectamine 2000. Lipofectamine 2000 was a more effective carrier (18.5%) than PAMAM G4 dendrimer (1.2%).

1. Introduction

Since they were first synthesized at the end of the 1970s (Flory, 1954; Buhleier et al., 1978; Tomalia et al., 1985; Newkome et al., 1985; Hawker and Fréchet, 1990), dendrimers have found their place in biology (Shcharbin et al., 2007a; Weber et al., 2008; Klajnert and Bryszewska, 2007). One of their promising applications is gene transfer: they have proved to be non-toxic and highly efficient carriers for delivering nucleic acids and short oligodeoxynucleotides (Shcharbin et al., 2007a; Weber et al., 2008; Klajnert and Bryszewska, 2007; Dufés et al., 2005). Such complexes have been called dendriplexes by analogy with polyplexes (polymer/nucleic acid complexes) and lipoplexes (liposome/nucleic acid complexes). Polyamidoamine (PAMAM) dendrimers (Tomalia et al., 1985) are based on an ethylenediamine core and branched units are built from methyl acrylate and ethylenediamine. The third, fourth, fifth and sixth generations of PAMAM-NH_2 dendrimers (PAMAM G3, G4, G5 and G6) possess 32, 64, 128 and 256 surface amino groups, respectively; their molecular weights are respectively 6.9, 14.2, 28.8 and 60 kDa, with corresponding molecular diameters 3.1, 4, 5.3 and 6.7 nm (Klajnert and Bryszewska, 2007). PAMAM G4-OH differs from PAMAM G4 by surface groups—it has 64 surface OH groups, which are neutral at pH 7.4. The structure of PAMAM-OH G4 dendrimer is presented in Fig. 1. PAMAM G4-25% has 75% NH_3^+ groups and 25% CH_3 groups; PAMAM G4-50% has 50% NH_3^+ groups and 50% CH_3 groups. The first attempts to analyze DNA delivery using PAMAM dendrimers with EDA cores were described in Haensler and Szoka (1993) and Kukowska-Latallo et al. (1996); PAMAM G2–G10 were shown to be effective delivery agents for transfecting different cell lines. Later, Steven Kuo and Lin (2007) showed that PAMAM G5 dendrimer was more efficient than PAMAM G2 (EDA core) for transfection with pDNA (pSG5lacZ), which encodes the lacZ gene for β-galactosidase, into human macrophage-like U937 and mouse fibroblast NIH/3T3 lines. Characterization of dendriplexes showed no clear correlation with transfection efficiency. Sometimes, a dendriplex was clearly observable by electron microscopy and gel-electrophoresis but showed low transfection efficiency (Haensler and Szoka, 1993; Kukowska-Latallo et al., 1996; Steven Kuo and Lin, 2007). The dependence of transfection efficiency on PAMAM dendrimer generation has a bell-shaped character. The transfection efficiency increases with increasing generation from 1st, reaches a maximum at 4–5th and decreases significantly by 9–10th (Haensler and Szoka, 1993; Kukowska-Latallo et al., 1996; Steven Kuo and Lin, 2007).

* Corresponding author. Fax: +375 17 284 23 59.
E-mail address: d.shcharbin@mail.ru (D. Shcharbin).

0378-5173/$ – see front matter © 2009 Elsevier B.V. All rights reserved.
doi:10.1016/j.ijpharm.2009.09.020

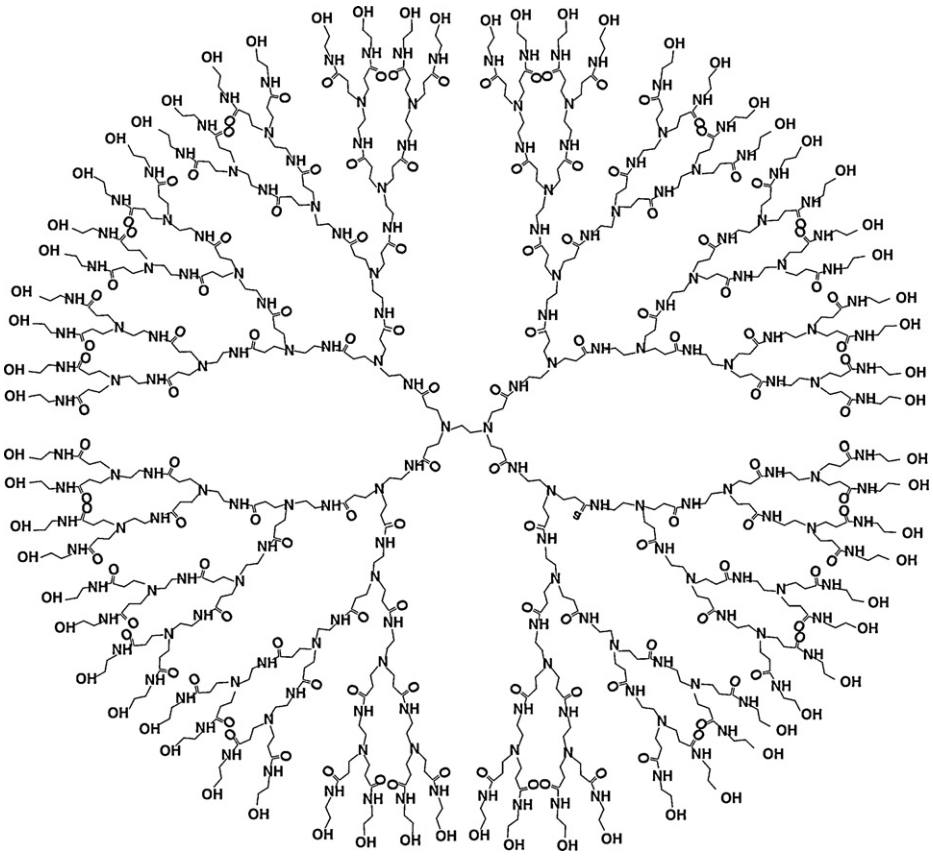

Fig. 1. Structure of PAMAM-OH G4 dendrimer (Tomalia et al., 1985).

The initial increase in transfection with dendrimer generation could be explained by the greater number of surface charges interacting with the nucleic acid, but the decrease of efficiency at high generations remained unclear. Haensler and Szoka (1993) explained this phenomenon in terms of decreased dendrimer flexibility; in the present paper we propose that it is due to increasing hydrophobicity. Also, one potential application of dendrimers is cell-based gene therapy involving the expression of neurotrophic factors. Transplantation of stem/precursor cells with engineered neurotrophin production may facilitate trophic support to recipients with neurotrauma, neurodegenerative diseases and other neural disorders. To demonstrate the feasibility of dendrimers in this field, we have used PAMAM G4 to modify mesenchymal stem cells from human bone marrow for neurotrophin-3 (NT-3) production.

2. Materials and methods

2.1. Ethidium bromide intercalation assay

The fluorescent dye ethidium bromide (EB) can intercalate into double-stranded DNA or RNA. It occupies an effective binding site of several base pairs, leading to a significant increase of its fluorescence intensity and to a blue-shift of its maximum emission wavelength (λ_{max}^{em}). Compounds with higher affinity for DNA (e.g. dendrimers) displace the dye, quench its fluorescence and induce a red-shift of its λ_{max}^{em}. EB was added to pGFP solution at a concentration of 1 molecule of dye per 1 bp of DNA and its fluorescence was monitored using a JASCO-FP 6300 spectrofluorimeter (JASCO GmbH, Germany). The excitation wavelength was 477 nm; the excitation and emission slits were 10 nm. The emission spectra were recorded between 500 and 700 nm and the position of emission maximum was determined. The 'dye-pGFP' complex was then titrated with a dendrimer and changes in the fluorescence parameters (intensity and λ_{max}^{em}) were recorded (Shcharbin et al., 2009).

The data were analyzed in terms of the apparent dendrimer-pGFP binding (association) constants using the equation:

$$\frac{1}{K_{ass}^{Dendrimer}} = \frac{IC_{50}}{1 + [EB] \cdot K_{ass}^{EB}} \quad (1)$$

where $K_{ass}^{Dendrimer}$ is the dendrimer association constant, IC_{50} is the concentration of dendrimer necessary to displace 50% of EB, [*EB*] is the total concentration of EB and K_{ass}^{EB} is the association constant for EB (Cheng and Prusoff, 1973; Klotz, 1985). In 50 mM Tris–HCl buffer (pH 6.35), K_{ass}^{EB} for ctDNA is $6.26 \times 10^5\ M^{-1}$ (Pang et al., 2007). K_{ass}^{EB} for pGFP is unknown.

To calculate the constants, the data graphs were modified so that the changes in fluorescence intensity of the EB-ctDNA complex when dendrimers were added were presented as

$$F^{rev} = \frac{F^{complex} - F^{pureEB}}{F_0^{complex} - F^{pureEB}} \quad (2)$$

where $F^{complex}$ is the fluorescence of EB-ctDNA in the presence of dendrimer, F^{pureEB} is the fluorescence of pure (free) EB, and $F_0^{complex}$ is the fluorescence of the EB-ctDNA complex in the absence of dendrimer when EB is fully bound by the ctDNA.

2.2. Fluorescence of l-anilinonaphthalene-8-sulfonic acid

ANS (l-anilinonaphthalene-8-sulfonic acid) was added to a PAMAM dendrimer solution at a ratio of 1 molecule per 5 molecules of dendrimer (the probe molecule is fully bound by dendrimer molecules for all dendrimers studied) and its fluorescence was monitored using a JASCO-FP 6300 spectrofluorimeter (JASCO

GmbH, Germany). The excitation wavelength was 370 nm; the excitation and emission slits were 5 nm. The ANS fluorescence emission spectra were recorded between 400 and 600 nm and the position of the emission maximum was determined.

2.3. Vector construction and preparation

Experiments to study the transfection efficiencies of different generations and modifications of dendrimers were performed using the plasmid vector pAAV-IRES-hrGFP (referred to here as pGFP, from Stratagene). To provide neurotrophin-3 expression, we inserted the human *ntf3* sequence (821 b.p.) into pGFP at the restriction sites ClaI and EcoRI (recognition sequences were added to the 5' termini of the amplification primers) by routine molecular cloning procedures. The resulting vector, designated pNTF3-IRES-hrGFP, was confirmed by restriction digest mapping and sequence analysis. Both the pGFP and pNTF3-IRES-hrGFP plasmids were propagated in *E. coli* strain DH5α and isolated by Plasmid Maxi kits (Qiagen) according to the manufacturer's instructions. Purified plasmid DNA with an A_{260}/A_{280} ratio of 1.8 was used for transfection.

2.4. Cell culture

Human embryonic kidney 293T cells (HEK 293T) and human bone marrow mesenchymal stem cells (hMSCs) were grown in DMEM-Glutamax (Gibco) with 10% heat-inactivated FBS (HyClone). Cells were routinely maintained on plastic tissue culture flasks and plates (Falcon) at 37 °C in a humidified atmosphere containing 5% CO_2/95% air. Adult human bone marrow was harvested from routine surgical procedures (pelvic osteotomies) with informed consent, diluted 10-fold in phosphate-buffered saline (PBS) and separated by centrifugation on a Ficoll-Paque layer. After centrifugation at 3000 × g for 30 min, the mononuclear cell layer was recovered from the gradient interface and washed with PBS. The cells were then centrifuged at 1500 × g for 30 min and resuspended in complete culture medium. The hMSC phenotype was confirmed by FACS analysis with CD90 and CD105 (positive), as well as CD34 and CD45 (negative), using a FACS-scan analytical flow cytometer (Becton Dickinson).

2.5. Transfection reagents

PAMAM-NH_2 G3, G4, G5 and G6 dendrimers (EDA core) were obtained from Dendritic NanoTechnologies (Mount Pleasant, Michigan, USA). Generation 4 PAMAM-OH dendrimers and PAMAM dendrimers with 25% and 50% hydrophobic chains (referred to here as PAMAM-25% and PAMAM-50%, respectively) were obtained from Sigma–Aldrich. Lipofectamine 2000 was obtained from Invitrogen (USA).

2.6. Transfection experiments

HEK 293T cells were seeded (3×10^4/well) in 24-well plates in 1 ml of medium. hMSCs (5×10^4 cells/well) were seeded in 6-well plates in 3 ml of medium. All cells were allowed to grow for 2–3 days before transfection to 65–70% confluence. For HEK 293T transfection, complexes of plasmid DNA (2 μg) and each of the dendrimers (G3, G4, G5 and G6) at a charge ratio of 1:1 were prepared in 100 μl 150 mM NaCl and the mixtures were incubated for 15 min at room temperature. For the hMSC wells, 10 μg plasmid DNA was diluted in 200 μl 150 mM NaCl. The medium was replaced with FBS-free medium before transfection. Following 2.5 h treatment of the DNA-dendrimer complexes, the medium was replaced with DMEM-Glutamax (Gibco) containing 10% heat-inactivated FBS. hMSCs were transfected with Lipofectamine 2000 in serum-free medium according to the manufacturer's instructions. hrGFP fluorescence was monitored by microscopy, and the percentage GFP-positive cells was determined after fixation with 2% paraformaldehyde using a FACS-scan analytical flow cytometer (Becton Dickinson).

2.7. Neurotrophin release

Secretion of NT3 protein into the culture supernatant was assessed *in vitro* using an enzyme-linked immunosorbent assay (ELISA). Medium samples were collected on the 1st, 3rd, 6th and 10th days after transfection and analyzed using NT-3 E_{max}® ImmunoAssay Systems (Promega, USA) according to the manufacturer's instructions. Three replicate samples from each well were pooled for statistical analysis.

3. Results

3.1. Ethidium bromide intercalation

Fig. 2 shows the changes in fluorescence emission intensity of EB complexed with pGFP after addition of PAMAM G3–G6 dendrimers at different charge ratios. For visualization, the intensities of pure EB and EB-PGFP complex were presented at point $X = 0.01$ instead of point $X = 0$ (Fig. 2). Addition of PAMAM G3–G6 and PAMAM G4-25% dendrimers in charge ratios from 0.1 to 2 led to a decrease of fluorescence intensity to the level of pure EB. This indicates the formation of dendriplexes. At higher charge ratios (2–15) the EB fluorescence was equal in intensity to that of pure EB. This means that the pGFP-dendrimer complex forms at charge ratios ~1:1 for PAMAM G3–G6 and at ~1:2 for PAMAM G4-25%. In contrast, PAMAM G4-50% formed a complex at charge ratio ~1:100. This means that its constant of association is significantly less than those of PAMAM G3–G6 and PAMAM G4-25%. Finally, PAMAM G4-OH had no effect on binding between EB and pGFP.

From Fig. 2 we determined the IC_{50} values for PAMAM G3–G6, PAMAM G4-25% and PAMAM G4-50% dendrimers on a charge ratio scale (Fig. 3). IC_{50} is the dendrimer/pGFP charge ratio at $F^{rel} = 0.5$. The charge ratio values can be easily transformed to molar ratios or concentrations. Unfortunately, K_{ass}^{EB} for pGFP is unknown and we cannot resolve $K_{ass}^{Dendrimer}$. However, as follows from Eq. (1):

$$K_{ass}^{Dendrimer} = \frac{const}{IC_{50}}$$

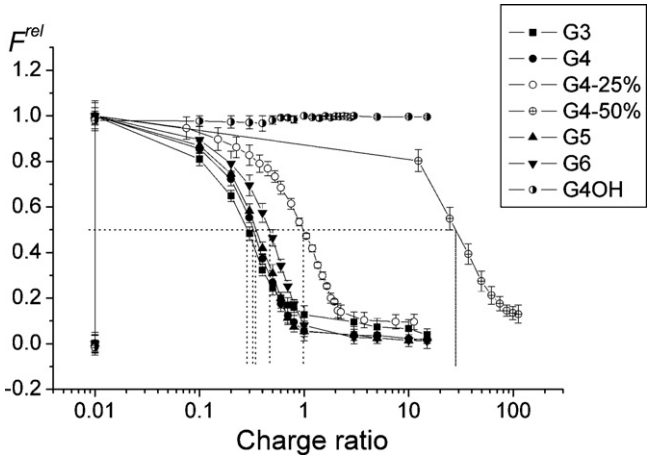

Fig. 2. The changes of fluorescence emission intensity of EB complexed with pGFP upon addition of PAMAM G3–G6 dendrimers at different charge ratios. $\lambda_{exc.} = 477$ nm. Data are mean ± S.E.M. of six independent experiments.

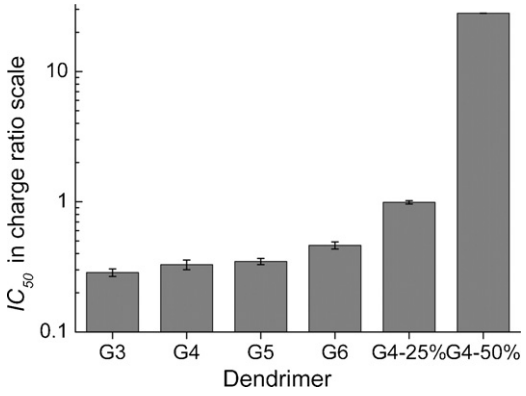

Fig. 3. The values of IC_{50} (at $F^{rel} = 0.5$) for PAMAM G3–G6 and PAMAM G4-25% dendrimers on the charge ratio scale. For details see Fig. 1. Data are mean ± S.E.M. Statistical analysis was performed by one-way ANOVA with post hoc analysis by the Newman–Keuls test.

where $const = (1 + [EB] \times K_{ass}^{EB})$. Thus, the smaller the IC_{50}, the higher the K_{ass}, so we can compare the IC_{50} values of dendrimers. Using one-way ANOVA and the post-hoc Newman–Keuls test, we found significant differences ($p < 0.01$) between PAMAM G6 and PAMAM G3–G5 dendrimers, between PAMAM G4-25% and PAMAM G3–G6 ($p < 0.01$), and between PAMAM G4-50% and PAMAM G4-OH and all other dendrimers ($p < 0.001$).

3.2. Fluorescence of ANS

ANS was added to a PAMAM dendrimer solution at a concentration ratio of 1 molecule of dye per 5 molecules of dendrimer (final concentration of ANS was 2 μmol/l) and its fluorescence was monitored. The results are presented in Fig. 4. The addition of an equal amount of dendrimer led to an increase of ANS fluorescence and the λ_{max} of emission was blue-shifted: λ_{max}^{em} of pure ANS in 0.15 M Tris–HCl, pH 7.4, was 500 ± 2 nm; λ_{max}^{em} of ANS complexed with G3 was 486 ± 3 nm, with G4 was 485 ± 2 nm, with G5 was 485 ± 2 nm, with G6 was 484 ± 2 nm, with G4-OH was 500 ± 2 nm, with G4-25% was 474 ± 2 nm, and with G4-50% was 473 ± 2 nm. Using one-way ANOVA and the post-hoc Newman–Keuls test we found a significant difference ($p < 0.05$) for practically all dendrimers except between the pairs pure ANS – G4-OH and G4-OH – G3.

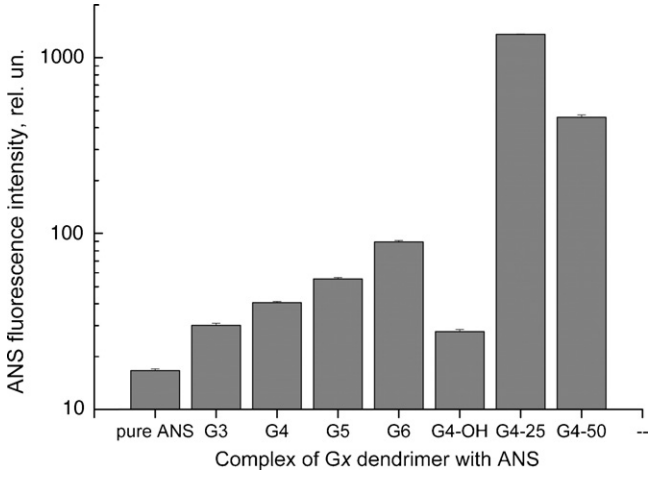

Fig. 4. Fluorescence intensities of pure ANS and ANS in complex with PAMAM dendrimers. $\lambda_{ex.} = 370$ nm, $\lambda_{em.} = 480$ nm. [PAMAM] = 50 μmol/l. [ANS] = 10 μmol/l. Statistical analysis was performed by one-way ANOVA with post-hoc analysis by the Newman-Keuls test.

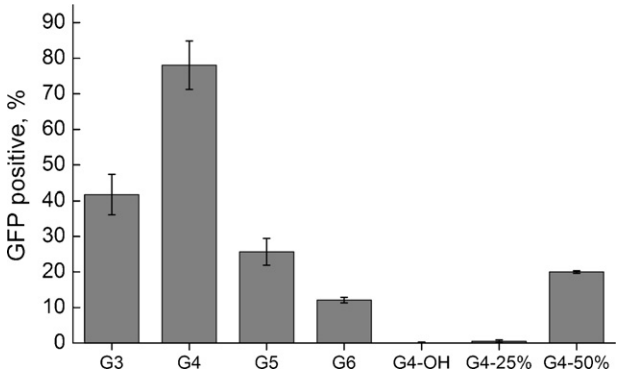

Fig. 5. Efficiency of transfection of pGFP by PAMAM G3–G6 dendrimers in HEK 293T cells. Data are mean ± S.D. of six experiments.

3.3. Efficiency of transfection

To compare the transfection efficiencies of several generations of dendrimers we used HEK 293T cells as a common standard for a variety of transfection agents. The transfection results are presented in Fig. 5. PAMAM G4 gave the highest level of transfection, reaching 78 ± 6.8% (mean ± S.D.) of cells. PAMAM G3 transfected 41.7 ± 5.6% of cells, PAMAM G5 25.69 ± 3.8%, PAMAM G6 13.1 ± 0.78%, and PAMAM G4-25% 0.1 ± 0.7%. PAMAM G4-OH showed zero transfection efficiency. Unexpectedly, PAMAM G4-50% showed a transfection efficiency of 20.00 ± 3.8%. The mean fluorescence intensity (MFI) of the transfected cells, indicating the level of expression of the reporter gene GFP, did not differ significantly between dendrimer generations (1075 ± 180 a.u. for G3, 1387 ± 191 a.u. for G4, 1498 ± 239 a.u. for G5 and 1396 ± 126 a.u. for G6).

3.4. Correlation between transfection and biophysical assays

Transfection efficiency correlated with IC_{50} for the group PAMAM G3–G5, and for the single dendrimers PAMAM G6 and PAMAM G4-25% (Fig. 6A, linear fit, $R = -0.78$, $p = 0.112$). Transfection efficiency correlated with dendrimer hydrophobicity, estimated by ANS fluorescence, for the group PAMAM G3–G5 and for the single dendrimers PAMAM G6 and PAMAM G4-25% (Fig. 6B, linear fit, $R = -0.81$, $p = 0.1$). The ethidium bromide intercalation and ANS fluorescence results correlated for PAMAM G3–G6 and PAMAM G4-25% dendrimers (Fig. 6C, $R = 0.99946$, $p < 0.001$).

3.5. Transfection by PAMAM dendrimers in hMSC

In the second stage of our studies we compared the transfection of pGFP by PAMAM dendrimers in hMSCs. The transfection results are presented in Fig. 7. G4/pGFP dendriplex, the most effective in HEK 293T cells with an approximately 80% transfection rate, gave 6.43% GFP-positive hMSCs, with MFI of 1054 ± 209 a.u. The transfection results for other dendrimers in hMSCs generally followed the trend shown by HEK cells, with efficiencies markedly lower than that of G4 dendrimer. The transfection rates in hMSC were 0.29% for the G3/pGFP dendriplex (MFI 1260 ± 161 a.u.), 0.21% for G5/pGFP (MFI 742 ± 383 a.u.) and 0.11% for G6/pGFP (MFI 538 ± 358 a.u.). The modified PAMAM G4 dendrimers (G4-OH, G4-25% and G4-50%) were unable to transfect hMSC.

3.6. Transfection of neurotropin-encoding plasmid into human MSCs

In the third stage we studied the ability of our most effective dendrimer carrier to deliver the neurotrophin-encoding plasmid

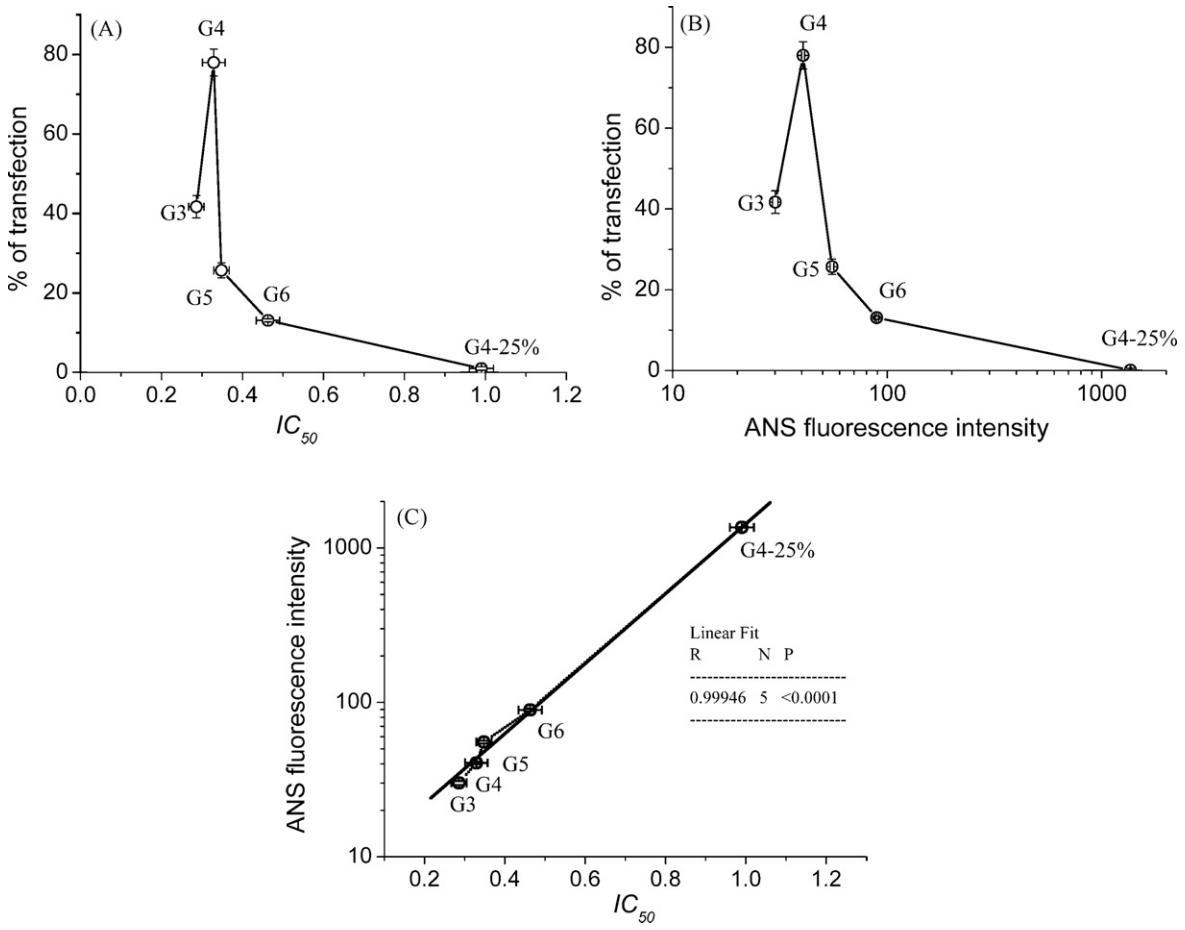

Fig. 6. The correlation between IC_{50} of dendrimers and their transfection efficiencies. Data are mean ± S.E.M.

pNTF3-IRES-hrGFP into human MSCs. PAMAM-NH_2 G4 dendrimer was used to transfect MSCs, and the release of neurotrophin into the culture medium was measured. Commercial Lipofectamine 2000 was used for comparison.

One-day post-transfection, the mean secretion levels of G4 dendrimer- and Lipofectamine-transfected hMSCs were 217 and 764 pg/ml, respectively (Fig. 8), reflecting the difference in transfection rates (1.2% for PAMAM-NH_2 G4 vs 18.5% for Lipofectamine 2000). No such difference was found in HEK 293T, where the secretion levels were 2.92 and 3.17 ng/ml for G4 dendrimer- and Lipofectamine-mediated delivery, with mean transfection efficiencies of 79% and 94%, respectively. In hMSCs, the difference in NT-3 secretion between the two transfection vehicles was statistically significant (one-way ANOVA, $p < 0.01$).

4. Discussion

4.1. Part A. Hydrophobicity of dendrimers and transfection

When PAMAM G3–G6 dendrimers were mixed in solution with pGFP, a stable complex was formed in which the DNA was bound to the dendrimer by electrostatic forces. The EB intercalation assay showed that the complexes formed at a charge ratio of 1:1 for

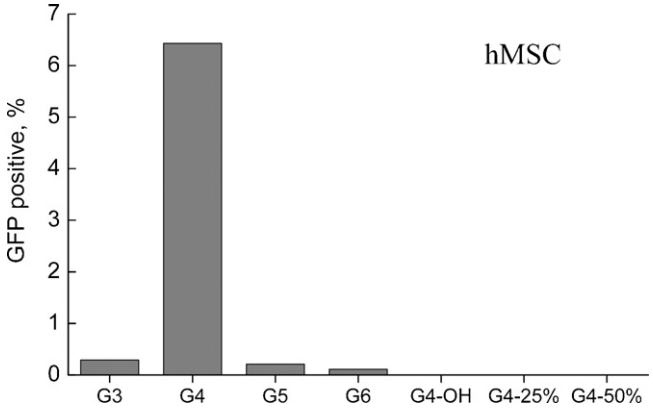

Fig. 7. Efficiency of transfection of pGFP by PAMAM G3–G6 dendrimers in hMSC cells. Data are mean ± S.D. of six experiments.

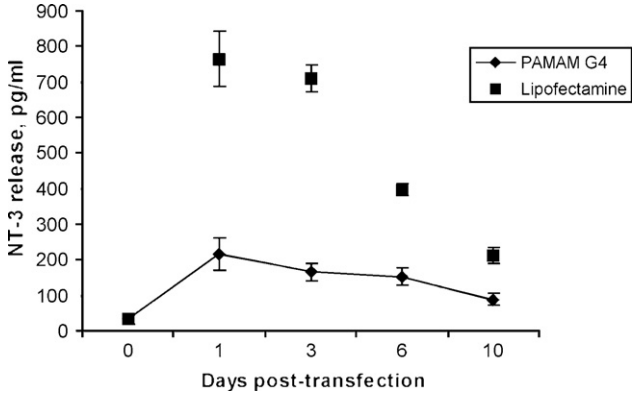

Fig. 8. NT-3 secretion into culture supernatant by hMSCs transfected with pNTF3-IRES-hrGFP plasmid by PAMAM-NH_2 G4 dendrimer and Lipofectamine 2000.

PAMAM G3–G6. This means that one molecule of pGFP (6100 b.p.) bound 381 molecules of PAMAM G3 dendrimer (381×32 NH_3^+ groups), 190 molecules of PAMAM G4 (190×64 NH_3^+ groups), 95 molecules of PAMAM G5 (95×128 NH_3^+ groups) and 47 molecules of PAMAM G6 (47×256 NH_3^+ groups). For PAMAM G4-25% the charge ratio was ~1:2. This means that one molecule of pGFP can bind 506 molecules of PAMAM G4-25% (506×48 NH_3^+ groups). For PAMAM G4-50% the charge ratio increased drastically to 1:100. This means that pGFP can bind 76,200 molecules of PAMAM G4-50%. The most probable situation is binding of pGFP to the micelles formed by PAMAM G4-50%. This is in good agreement with the decrease of hydrophobicity of these micelles monitored by ANS (Fig. 4 and below) and the light scattering of samples at 650 nm. The light scattering of PAMAM G4-50% in solution increased significantly, indicating the formation of big micelles because of the low solubility of this dendrimer in buffer (data not presented). The cutoff size for efficient cellular uptake is anticipated to be ~200 nm (Wood et al., 2005). PAMAM G3, G4, G4-25%, G5 and G6 dendrimers have diameters of 3.1, 4, 4, 5.3 and 6.7 nm, respectively. The volume of a sphere with diameter 3.1 nm (PAMAM G3) is $(4/3)\pi(D/2)^3$, i.e. ~15.6 nm^3. The diameter of a sphere with volume (381×15.6 nm^3) is 22.5 nm. The same calculations for PAMAM G4, G4-25%, G5 and G6 dendrimers give us the diameters 23, 26, 24.1 and 24.2 nm, respectively. This means that complexes of one molecule of pGFP with molecules of G3–G6 and G4-25% have a minimal volume of ~23–26 nm. For PAMAM G4-50% the equivalent diameter is ~123 nm, still less than anticipated cut-off in transfection efficiency of complexes but much higher than for PAMAM G3–G6 and PAMAM G4-25%. The electron microscopic images of PAMAM G3–G6/pGFP dendriplexes (data not presented) show that the real volumes were greater than these calculated ones but smaller than the anticipated cutoff for efficient cellular uptake.

The dendrimers showed completely different transfection efficiencies. We can explain this as follows. First of all, we should exclude PAMAM G4-OH from consideration. It follows from the data that the neutral charge of PAMAM G4-OH meant no interaction with pGFP or competition with EB for pGFP binding sites (see Fig. 2). The interaction between PAMAM G4-OH dendrimer and ANS gave a similar picture. In 0.15 Tris–HCl, pH 7.4, the conditions used, the pure hydrophobic ANS probe had a weak fluorescence over the range 400–600 nm with an emission maximum at ~500 nm. This is a consequence of its low fluorescence yield in a polar environment (Slavik, 1982). As we found earlier, the interaction between ANS and PAMAM dendrimers led to partial penetration into the dendrimers' hydrophobic cavities and a significant increase of fluorescence (Jokiel et al., 2007; Klajnert et al., 2007; Shcharbin et al., 2003, 2005, 2007b). At the 1:5 molar ratio of ANS to dendrimer used in the present experiments, all molecules of ANS are bound by PAMAM dendrimers and the fluorescence intensity of ANS is represented by molecules attached to the dendrimer surface and partially inserted in its cavities (Jokiel et al., 2007; Klajnert et al., 2007; Shcharbin et al., 2003, 2005, 2007b). In this case, ANS can be represented as a "monomer of DNA", i.e. a molecule with one anionic charge and a hydrophobic part. In our case the lack of positive charge on the G4-OH surface resulted in no interaction with ANS. The interaction between PAMAM G4-OH and pGFP gave a similar picture. Thus, PAMAM G4-OH did not form a dendriplex with pGFP and showed no transfection activity.

In the second stage we excluded PAMAM G4-50% from the range of PAMAM G3–G6 and PAMAM G4-25%. In view of its structure, PAMAM G4-50% is more hydrophobic than PAMAM G4-25%. Moreover, it is sufficiently hydrophobic to form micelles in solution. This follows (1) from the EB data (see Fig. 2), (2) from the decrease of binding with ANS (see Fig. 4) suggesting a decrease of hydrophobicity of its micelles, (3) from the light scattering data (not presented). The balance between hydrophobicity and charge allows the micelles of PAMAM G4-50% to have a higher transfection activity than PAMAM G4-25% or PAMAM G6. Nevertheless, the transfection efficiency of such micelles is still significantly less than that of pure PAMAM G4.

Finally, we obtained the range: PAMAM G3–G6 and hydrophobically modified PAMAM G4-25%. In these complexes, pure dendrimers attach to pGFP forming dendriplexes.

It is known that increase of dendrimer generation leads to more hydrophobic internal cavities (Svenson and Tomalia, 2005), so that together with more surface groups, the dendrimer becomes more hydrophobic. To our mind this is the main reason for the lower transfection efficiencies of high generations of PAMAM dendrimers. The interaction of DNA with a dendrimer is determined by two main factors: (1) electrostatic forces between the anionic phosphate groups of DNA and the cationic groups of the dendrimer, (2) hydrophobic interactions between the DNA chain and internal cavities of the dendrimer. Fig. 5 presents the interaction between the hydrophobic fluorescent probe ANS and PAMAM dendrimers and we can see the increase of ANS fluorescence intensity. Thus, the blue-shift of the ANS fluorescence emission maximum and the increase of fluorescence intensity in the presence of dendrimers reflect an increase in dendrimer hydrophobicity. This does not concern PAMAM G4-OH, which cannot bind ANS by electrostatic forces at its surface. The greater hydrophobicity of PAMAM G5 and G6 in comparison with G4 led to a lower transfection activity. PAMAM G6 competed significantly less effectively with EB for pGFP ($p < 0.01$) than PAMAM G3–G5 (Fig. 3). Both the lowering surface charge and the hydrophobic modification of PAMAM G4-25% made it compete significantly less effectively ($p < 0.01$) with EB for DNA (Fig. 3) and diminished its transfection efficiency (Fig. 5). Our results also explain the greater transfection efficiency of fractioned PAMAM dendrimers (Tang et al., 1996), known as the commercial preparation Superfect™. In such dendrimers, some branches are removed, increasing their flexibility. Also, the hydrophobic cavities of such dendrimers are destroyed. Our data agree well with those of Braun et al. (Braun et al., 2005), who used differential scanning calorimetry, FTIR and CD to evaluate the thermal stability of DNA complexed to PAMAM dendrimers. FTIR showed a decreased frequency of the antisymmetric phosphate stretch (1223 cm^{-1}) when PAMAM dendrimer was added, suggesting that this moiety was directly involved in the dendrimer/DNA interaction, presumably through direct electrostatic interaction with the dendrimer amino groups. For high generations (7 and 9), however, the positions of the vibrations arising from both backbone and bases were shifted, suggesting some direct dendrimer/DNA interaction in addition to the expected phosphate–amine electrostatic interactions. A possible increase of hydrophobic DNA-dendrimer interactions at high generations of PAMAM dendrimers was discussed (Braun et al., 2005). The proposal of dendrimer hydrophobicity is in good agreement with results on complexation between DNA and surface-neutral and internally-cationic PAMAM dendrimers into which pDNA can penetrate (Lee et al., 2003), and with the increased capacity for aggregation of complexes between DNA and higher generations of PAMAM dendrimers (Bielinska et al., 1997) (and for PAMAM G4-50%, increased hydrophobicity leads to aggregation/micellation).

What accounts for the correlation between the hydrophobicity and transfection efficiency of a dendrimer? Seemingly, by analogy with liposomes (Chiaramoni et al., 2007, 2008), dendrimer hydrophobicity affects DNA conformation. Chiaramoni et al. (2008) showed that DNA lyophilized with highly hydrophobic cationic vesicles changed its conformation into a more condensed form, probably the C form. Marty et al. (2009) studied the stability of lipid–DNA complexes and found that more stable DNA adducts formed with cationic lipids than with neutral lipids. Patel and Anchordoquy (2005) showed that the acyl chain made a major contribution to binding between DNA and lipospermine in com-

parison with spermine (the significant impact of hydrophobic interactions—$\Delta H_{nonelec}$). Zinselmeyer et al. (2002) found that DNA was fully condensed by higher generations of polypropyleneimine dendrimers (3rd–5th generations) but only partially condensed by lower generations (1st and 2nd), and the lower generations were more efficient for gene transfection.

Thus, a decrease of electrostatic interactions and more hydrophobic packing of DNA in PAMAM dendrimers can significantly reduce their capacity for gene transfection.

The second interesting point is a possible correlation between ethidium bromide intercalation and transfection efficiency. Chemists have synthesized many modified dendrimers and they need a tool for rapid screening of their transfection efficiencies. As follows from Fig. 3, the interaction between PAMAM dendrimers and pGFP studied by EB intercalation correlated negatively with their transfection efficiencies (Figs. 5 and 7). Transfection efficiency correlated with IC_{50} in HEK 293 cells for the group PAMAM G3–G5 and the single dendrimers PAMAM G6 and PAMAM G4-25% (Fig. 6A, linear fit, $R = -0.78$, $p = 0.112$); this was also found in hMSCs (data not presented). A similar picture – a negative correlation between EB intercalation and transfection – was observed by Tang and Szoka (1997). In their study, polymers mediating high transfection (fractured dendrimer and polyethylenimine) had minimal IC_{50} values on the charge ratio scale (Tang and Szoka, 1997). In Zhang et al. (2005), minimal IC_{50} values of trimesyl core dendrimers on the charge ratio scale correlated with high transfection efficiencies in COS-7 cells and hepatocytes. Waite et al. (2009) found that acetylation of dendrimers reduced the delivery of siRNA into U-87 cells, which correlated negatively with IC_{50} values on the charge ratio scale. But no such correlation was observed in CHO-K1 cells (Braun et al., 2005). Thus, comparison of a newly synthesized dendrimer with a known dendrimer by the ethidium bromide intercalation assay seems to be qualitatively predictive of its transfection efficiency. The very good correlation ($R = 0.99946$, $p < 0.0001$) between the fluorescence intensities of two different probes that interact with dendrimers in different ways (dye displacement for EB, complexation for ANS) shows that by using two simple tests with EB and ANS and a known PAMAM dendrimer (for example G4), we can also predict the hydrophobicity of modified PAMAM dendrimers, their interactions with DNA and their ability to transfect cells. Seemingly, the same principle will apply to all dendrimers synthesized.

4.2. Part B. Transfection of neurotrophin-encoding plasmid into human MSCs

In last part of the present work we investigated the capacity of PAMAM dendrimers to deliver neurotrophin that could be expressed in human stem cells. Among the neurotrophins, we chose the well-studied human NT-3 encoded by *ntf3*. NT-3 protein is a member of the neurotrophin family, which controls the survival and differentiation of mammalian neurons. NT-3 is also important in supporting the post-traumatic recovery of neural cells. Transplants of NT-3-transduced fibroblasts or neural stem cells rescued axotomized Clarke's nucleus neurons after spinal cord hemisection, while NGF-expressing transplants had only a partial effect (Himes et al., 2001). The transplantation of precursor cells expressing multineurotrophin with NT-3 properties promotes enhanced re-myelination and electrophysiological recovery after traumatic spinal cord injury (SCI) in rats (Ronsyn et al., 2007). Grafting of olfactory ensheathing glia transduced with adenovirus vectors encoding neurotrophin-3 (NT-3) reduced lesion volumes in animals with unilateral transection of the dorsolateral funiculus (Ruitenberg et al., 2005). Myelination by oligodendrocytes is also enhanced by NT3 in both neuronal cultures and injured CNS (Jean et al., 2003; Yan and Wood, 2000; McTigue et al., 1998). Over-expression of neurotrophin-3 also directs the differentiation of human MSCs to a neural lineage, as identified by the neural markers nestin, NF, MAP2 and PSD95 (Zhang et al., 2006). For NT-3 production in hMSCs, we constructed the pNTF3-IRES-hrGFP plasmid. The internal ribosome entry site (IRES) sequence from encephalomyocarditis virus (EMCV) upstream of the reporter, humanized recombinant green fluorescent protein (hrGFP), ensures expression of both NT-3 and hrGFP under the potent CMV promoter enhanced with the chicken β-globin intron. Simultaneous expression of hrGFP from the same transcript via the IRES-driven second open reading frame serves as a marker for both transfection efficiency and *ntf3* transgene expression. NT-3 secretion into the culture medium was assessed using a routine ELISA protocol. We found that both PAMAM and Lipofectamine vehicles delivered the pNTF3-IRES-hrGFP plasmid into hMSCs and NT-3 was secreted into the medium. hMSC transfection rates for pNTF3-IRES-hrGFP plasmid vector were 1.2% for PAMAM dendrimer and 18.5% for Lipofectamine 2000. The neurotrophin release level after transfection with either vehicle generally agreed well with the data on plasmid-based NT-3 expression in human MSCs by Ronsyn and co-workers (Himes et al., 2001).

We also studied the 10-day dynamics of neurotrophin release. Fig. 7 shows that NT-3 secretion gradually decreased with time but still remained well above control (32.5 pg/ml) on day 10 for both vehicles. Transient expression of neurotrophins makes neurons complete their differentiation in development and contributes to neuronal survival and possibly post-traumatic recovery (Coppola et al., 2001; Farinas et al., 2001; Reichardt, 2006).

5. Conclusions

PAMAM G4 has a higher transfection efficiency than PAMAM G3–G6, G4-OH, G4-25% or G4-50% dendrimers for HEK 293 cells and human mesenchymal stem cells. It was concluded that more hydrophobic dendrimers had lower transfection abilities. PAMAM G4-50% is highly hydrophobic and forms micelles in solution, which are able to transfect pGFP. Ethidium bromide intercalation correlated with transfection efficiency for PAMAM dendrimers. Lipofectamine 2000 was a more effective carrier (18.5%) than PAMAM G4 dendrimer (1.2%) for a neurotropin-encoding plasmid in mesenchymal stem cells.

Acknowledgement

This work has been supported by grant from ERA-NET NAN2007-31198-E.

References

Bielinska, A.U., Kukowska-Latallo, J.F., Baker, J.R., 1997. The interaction of plasmid DNA with polyamidoamine dendrimers: mechanism of complex formation and analysis of alterations induced in nuclease sensitivity and transcriptional activity of the complexed DNA. Biochim. Biophys. Acta 1353, 180–190.

Braun, C.S., Vetro, J.A., Tomalia, D.A., Koe, G.S., Koe, J.G., Middaugh, C.R., 2005. Structure/function relationships of polyamidoamine/DNA dendrimers as gene delivery vehicles. J. Pharm. Sci. 94, 423–436.

Buhleier, E.W., Wehner, W., Vögtle, F., 1978. "Cascade"- and "nonskid-chain-like" syntheses of molecular cavity topologies. Synthesis 2, 155–158.

Cheng, Y.C., Prusoff, W.H., 1973. Relationship between the inhibition constant (KI) and the concentration of inhibitor which causes 50 per cent inhibition (I50) of an enzymatic reaction. Biochem. Pharmacol. 22, 3099–3108.

Chiaramoni, N.S., Speroni, L., Taira, M.C., del, S., Alonso, V., 2007. Liposome/DNA systems: correlation between association, hydrophobicity and cell viability. Biotechnol. Lett. 29, 1637–1644.

Chiaramoni, N.S., Baccarini, L.C., Taira, M.C., del, S., Alonso, V., 2008. Liposome/DNA Systems: Correlation Between Hydrophobicity and DNA Conformational Changes, 34.

Coppola, V., Kucera, J., Palko, M.E., Martinez-De Velasco, J., Lyons, W.E., Fritzsch, B., Tessarollo, L., 2001. Dissection of NT3 functions in vivo by gene replacement strategy. Development 128, 4315–4327.

Dufés, Ch., Uchegbu, I.F., Schätzlein, A.G., 2005. Dendrimers in gene delivery. Adv. Drug Deliv. Rev. 57, 2177–2202.

Farinas, I., Jones, K.R., Tessarollo, L., Vigers, A.J., Huang, E., Kirstein, M., de Caprona, D.C., Coppola, V., Backus, C., Reichardt, L.F., Fritzsch, B., 2001. Spatial shaping of cochlear innervation by temporally regulated neurotrophin expression. J. Neurosci. 21, 6170–6180.

Flory, P.J., 1954. Molecular size distribution in three dimensional polymers. VI. Branched polymers containing A-R-B_{f-1} type units. J. Am. Chem. Soc. 74, 2718–2723.

Haensler, J., Szoka, F.C., 1993. Polyamidoamine cascade polymers mediate efficient transfection of cells in culture. Bioconjug. Chem. 1093, 372–379.

Hawker, C.J., Fréchet, J.M.J., 1990. Preparation of polymers with controlled molecular architecture. A new convergent approach to dendritic macromolecules. J. Am. Chem. Soc. 112, 7638–7647.

Himes, B.T., Liu, Y., Solowska, J.M., Snyder, E.Y., Fischer, I., Tessler, A., 2001. Transplants of cells genetically modified to express neurotrophin-3 rescue axotomized Clarke's nucleus neurons after spinal cord hemisection in adult rats. J. Neurosci. Res. 65, 549–564.

Jean, I., Lavialle, C., Barthelaix-Pouplard, A., Fressinaud, C., 2003. Neurotrophin-3 specifically increases mature oligodendrocyte population and enhances remyelination after chemical demyelination of adult rat CNS. Brain Res. 972, 110–118.

Jokiel, M., Shcharbin, D., Janiszewska, J., Urbanczyk-Lipkowska, Z., Bryszewska, M., 2007. The interaction between polycationic poly-lysine dendrimers and charged and neutral fluorescent probes. J. Fluorescence 17, 73–79.

Klajnert, B., Bryszewska, M., 2007. Dendrimers in Medicine. Nova Science Pub, N.-Y, 141 p.

Klajnert, B., Pastucha, A., Shcharbin, D., Bryszewska, M., 2007. Binding properties of polyamidoamine pendrimers. J. Appl. Polym Sci. 103, 2036–2040.

Klotz, I.M., 1985. Ligand–receptor interactions: facts and fantasies. Q. Rev. Biophys. 18, 227–259.

Kukowska-Latallo, J.F., Bielinska, A.U., Johnson, J., Spindler, R., Tomalia, D.A., Baker, J.R., 1996. Efficient transfer of genetic material into mammalian cells using starburst polyamidoamine dendrimers. Proc. Natl. Acad. Sci. 93, 4897–4902.

Lee, J.H., Lim, Y.B., Choi, J.S., Lee, Y., Kim, T.I., Kim, H.J., Joon, J.K., Kim, K., Park, J.S., 2003. Polyplexes assembled with internally quaternized PAMAM-OH dendrimer and plasmid DNA have a neutral surface and gene delivery potency. Bioconjug. Chem. 14, 1214–1221.

Marty, R., N'soukpoé-Kossi, C.N., Charbonneau, D., Weinert, C.M., Kreplak, L., Tajmir-Riahi, H.-A., 2009. Structural analysis of DNA complexation with cationic lipids. Nucleic Acids Res. 37, 849–857.

McTigue, D.M., Horner, P.J., Stokes, B.T., Gage, F.H., 1998. Neurotrophin-3 and brain-derived neurotrophic factor induce oligodendrocyte proliferation and myelination of regenerating axons in the contused adult rat spinal cord. J. Neurosci. 18, 5354–5365.

Newkome, G.R., Yao, Z., Baker, G.R., Gupta, V.K., 1985. Cascade molecules: a new approach to micelles. A [27]-arborol. J. Org. Chem. 50, 2003–2004.

Pang, J.-Y., Long, Y.-H., Chen, W.-H., Jiang, Z.-H., 2007. Amplification of DNA-binding affinities of protoberberine alkaloids by appended polyamines. Bioorg. Med. Chem. Lett. 17, 1018–1021.

Patel, M.M., Anchordoquy, T.J., 2005. Contribution of hydrophobicity to thermodynamics of ligand-DNA binding and DNA collapse. Biophys. J. 88, 2089–2103.

Reichardt, L.F., 2006. Neurotrophin-regulated signalling pathways. Philos. Trans. R. Soc. Lond. B Biol. Sci. 361, 1545–1564.

Ronsyn, M.W., Daans, J., Spaepen, G., Chatterjee, S., Vermeulen, K., D'Haese, P., Van Tendeloo, V.F., Van Marck, E., Ysebaert, D., Berneman, Z.N., Jorens, P.G., Ponsaerts, P., 2007. Plasmid-based genetic modification of human bone marrow-derived stromal cells: analysis of cell survival and transgene expression after transplantation in rat spinal cord. BMC Biotechnol. 7, 90–107.

Ruitenberg, M.J., Levison, D.B., Lee, S.V., Verhaagen, J., Harvey, A.R., Plant, G.W., 2005. NT-3 expression from engineered olfactory ensheathing glia promotes spinal sparing and regeneration. Brain 128, 839–853.

Shcharbin, D., Klajnert, B., Mazhul', V., Bryszewska, M., 2003. Estimation of PAMAM dendrimers binding capacity by fluorescent probe ANS. J. Fluorescence 13, 519–524.

Shcharbin, D., Klajnert, B., Mazhul, V., Bryszewska, M., 2005. Dendrimer interactions with hydrophobic fluorescent probes and human serum albumin. J. Fluorescence 15, 21–29.

Shcharbin, D., Pedziwiatr, E., Chonco, L., Bermejo-Martín, J.F., Ortega, P., de la Mata, F.J., Eritja, R., Gómez, R., Klajnert, B., Bryszewska, M., Muñoz-Fernandez, M^{a}.A., 2007a. Analysis of interaction between dendriplexes and bovine serum albumin. Biomacromolecules 8, 2059–2062.

Shcharbin, D., Szwedzka, M., Bryszewska, M., 2007b. Does fluorescence of ANS reflect its binding to PAMAM dendrimers? Bioorg. Chem. 35, 170–174.

Shcharbin, D., Pedziwiatr, E., Bryszewska, M., 2009. How to Study Dendriplexes I: characterization. J. Controlled Release 135, 186–197.

Slavik, J., 1982. Anilinonaphthalene sulfonate as a probe of membrane composition and function. Biochim. Biophys. Acta 694, 1–25.

Steven Kuo, J.-H., Lin, Y.-L., 2007. Remnant cationic dendrimers block RNA migration in electrophoresis after monophasic lysis. J. Biotechnol. 129, 383–390.

Svenson, S., Tomalia, D.A., 2005. Dendrimers in biomedical applications—reflections on the field. Adv. Drug Del. Rev. 57, 2106–2129.

Tang, M.X., Szoka, F.C., 1997. The influence of polymer structure on the interactions of cationic polymers with DNA and morphology of the resulting complexes. Gene Therapy 4, 823–832.

Tang, M.X., Redemann, C.T., Szoka Jr., F.C., 1996. In vitro gene delivery by degraded polyamidoamine dendrimers. Bioconjug. Chem. 7, 703–714.

Tomalia, D.A., Baker, H., Dewald, J.R., Hall, M., Kallos, G., Martin, S., Roeck, J., Ryder, J., Smith, P., 1985. A new class of polymers: starburst dendritic macromolecules. Polym. J. 17, 117–132.

Waite, C.L., Sparks, S.M., Uhrich, K.E., Roth, C.M., 2009. Acetylation of PAMAM dendrimers for cellular delivery of siRNA. BMC Biotechnol. 9 (38), 1–10.

Weber, N., Ortega, P., Clemente, M.I., Shcharbin, D., Bryszewska, M., de la Mata, F.J., Gómez, R., Muñoz-Fernández, M.A., 2008. Characterization of carbosilane dendrimers as effective carriers of siRNA to HIV infected lymphocytes. J. Controlled Release 132, 55–64.

Wood, K.C., Little, S.R., Langer, R., Hammond, P.T., 2005. A family of hierarchically self-assembling linear-dendritic hybrid polymers for highly efficient targeted gene delivery. Angew. Chem. Int. Ed. 44, 6704–6708.

Yan, H., Wood, P.M., 2000. NT-3 weakly stimulates proliferation of adult rat O1(−)O4(+) oligodendrocyte-lineage cells and increases oligodendrocyte myelination in vitro. J. Neurosci. Res. 62, 329–335.

Zhang, X.-Q., Wang, X.-L., Huang, S.-W., Zhuo, R.-X., Liu, Z.-L., Mao, H.-Q., Leong, K.W., 2005. In vitro gene delivery using polyamidoamine dendrimers with a trimesyl core. Biomacromolecules 6, 341–350.

Zhang, W., Zeng, Y.S., Zhang, X.B., Wang, J.M., Zhang, W., Chen, S.J., 2006. Combination of adenoviral vector-mediated neurotrophin-3 gene transfer and retinoic acid promotes adult bone marrow cells to differentiate into neuronal phenotypes. Neurosci. Lett. 408, 98–103.

Zinselmeyer, B.H., Mackay, S.P., Schatzlein, A.G., Uchegbu, I.F., 2002. The lower-generation polypropylenimine dendrimers are effective gene-transfer agents. Pharm. Res. 19, 960–967.